

# Development of a Suitable Physical Form for a Sphingosine-1-phosphate Receptor Agonist

Henry Morrison,<sup>\*,†</sup> Brenda Burke,<sup>‡</sup> Dennis Lei,<sup>§</sup> Vivian Robertson,<sup>†</sup> Karthik Nagapudi,<sup>†</sup> Johann Chan,<sup>‡</sup> Anu Gore,<sup>§</sup> Jan Fang,<sup>†</sup> and Jonan Jona<sup>†</sup>

<sup>†</sup>Amgen Inc., One Amgen Center Drive, Thousand Oaks, California 91320, United States

<sup>‡</sup>Gilead Inc., 333 Lakeside Dr, Foster City, California 94404, United States

<sup>§</sup>Allergan Inc., 2525 Dupont Drive, Irvine, California 92612, United States

**S** Supporting Information

**ABSTRACT:** AMG 369 (**1**), a novel S1P<sub>1</sub> agonist, was selected for clinical development for the treatment of multiple sclerosis. Form B of the zwitterionic molecule was initially identified as a potential development form. However, because of the instability of the phase as a function of ambient relative humidity, investigations of other polymorphs of the zwitterion and basic and acidic salt screening were conducted to identify an acceptable physical form for long-term development. An HCl dihydrate, an unsolvated sulfate salt, a hexahydrate calcium salt, and a monohydrate of the zwitterion were identified as potentially viable phases. The quality attributes of these phases were then compared along with their propensity to undergo acid-promoted degradation.

## INTRODUCTION

AMG 369 (**1**), a small molecule S1P<sub>1</sub> agonist, was selected for clinical development for the treatment of multiple sclerosis. Compound **1** causes lymphocyte sequestration in the secondary lymph organs and subsequent repression of the peripheral immune response (Figure 1).<sup>1</sup> The S1P<sub>1</sub> receptor has previously been shown to have impact on cardiovascular function, pulmonary endothelium integrity, and cell motility.<sup>2,3</sup> Consequently, an orally bioavailable S1P<sub>1</sub> agonist has therapeutic potential in multiple indications, including multiple sclerosis, rheumatoid arthritis, inflammatory bowel disease, and transplant rejection.<sup>4–6</sup>

The active pharmaceutical ingredient (API, **1**) was isolated as a zwitterion (form B) during early development. Although this phase was found to be crystalline via X-ray powder diffraction (XRPD) and the differential scanning calorimeter (DSC) curve indicated a high temperature melt around 183 °C, it was found to be physically unstable as a function of ambient relative humidity via moisture sorption analysis (Figure 2). Form B was found to reversibly convert to an unstable hydrate (form J) around a critical relative humidity of 45%. Because of this potential for lack of form control, development of form B was halted. Polymorph screening and the formation of crystalline salts is an approach used for optimization of physical properties such as melting point, hygroscopicity, chemical stability, dissolution rate, and crystal form.<sup>7–13</sup> As a result of the unsuitable nature of form B, a comprehensive polymorph/salt screening investigation was conducted in order to identify a crystalline form with acceptable physical characteristics for further development.

## RESULTS AND DISCUSSION

**Polymorph Screen.** A full polymorph screen was conducted on **1**, and up to nine forms were identified (Figures 3 and 4). Forms A, C, and D were deprioritized because they were poorly

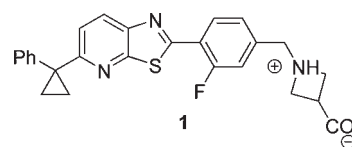


Figure 1. AMG 369 (**1**).

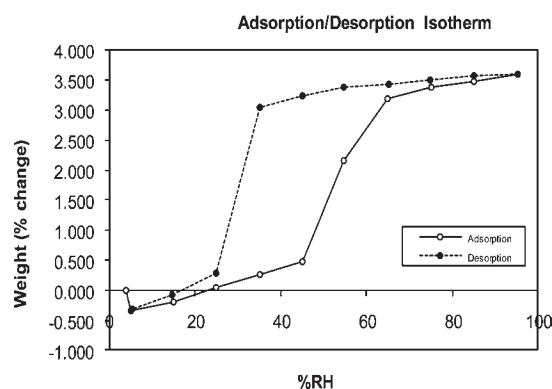


Figure 2. Moisture balance curve for zwitterionic form B.

crystalline phases that could not be reproduced, while form I was a crystalline phase but also not scalable. Forms B and J were no longer pursued for reasons previously discussed. Form E was an organic solvate and was not further pursued because of the high levels of residual solvent present. Form F was a monohydrate (Karl Fischer, KF = 3.5 wt %, theoretical 3.8 wt %) whose DSC

Received: July 18, 2011

Published: August 20, 2011

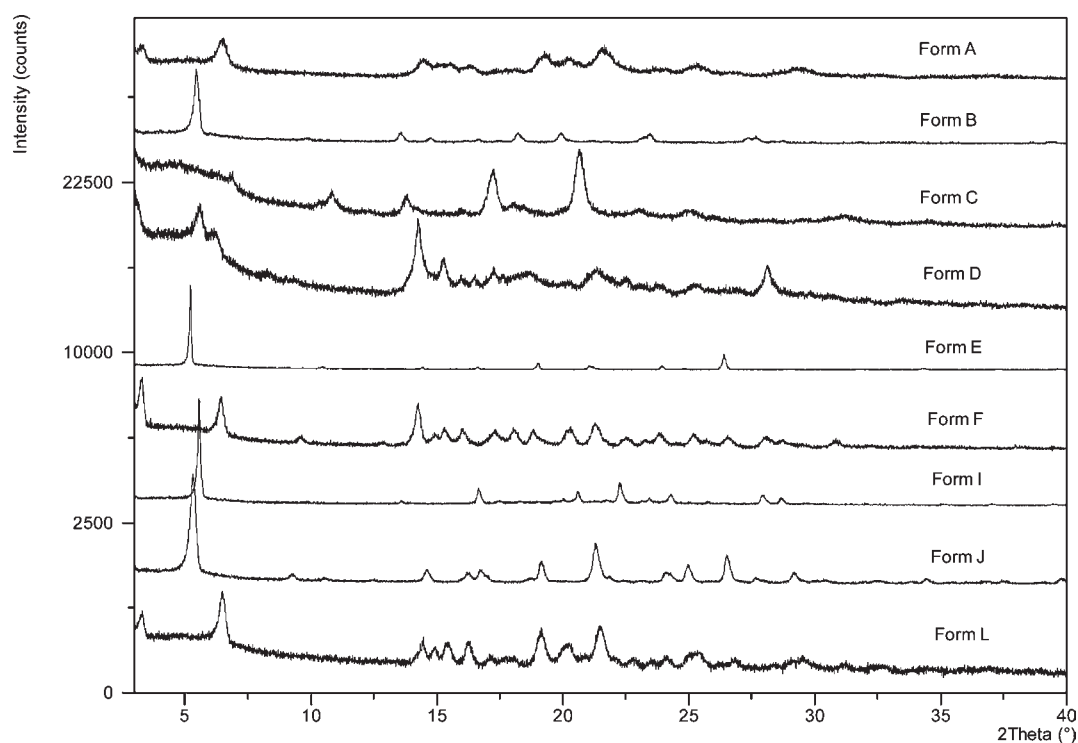


Figure 3. Summary of XRPD patterns from the zwitterion polymorph screen.

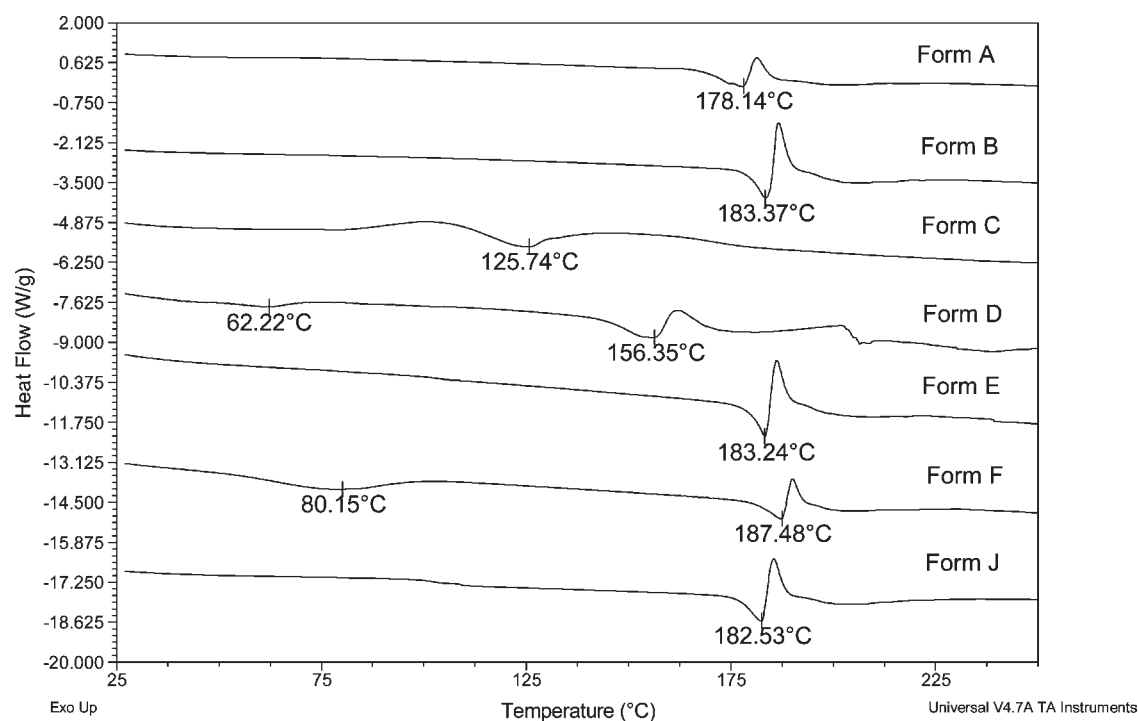
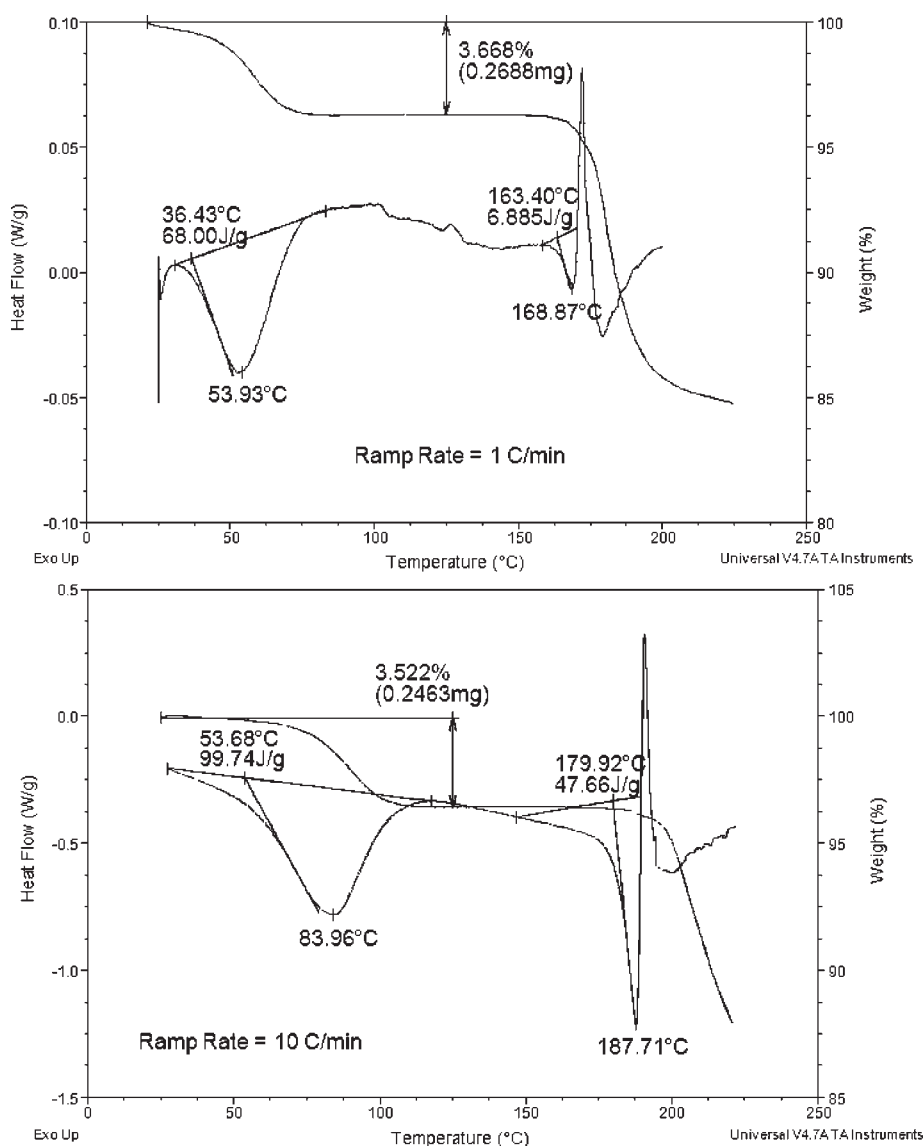


Figure 4. Summary of DSC curves from zwitterion polymorph screen.

curve indicated two endothermic transitions. The transition with a peak temperature of 80 °C was attributed to desolvation and confirmed by TGA analysis, while the transition with a peak temperature of ~187 °C was initially attributed to a melt. Upon desolvation, form F was found to convert to an unstable

unsolvated form (form L) that readily rehydrated back to the monohydrate when exposed to ambient conditions. Water vapor sorption analysis for form F indicated that the material is slightly hygroscopic, and only +1.75% weight change was observed at relative humidity (RH) as high as at 95%. The material lost this



**Figure 5.** Variable ramp rate DSC and TGA of zwitterionic form F.

weight upon returning to ambient conditions, and the phase remained unchanged post experiment based on XRPD results. Because form F was found to be a crystalline slightly hygroscopic monohydrate with a relatively high desolvation temperature, it was selected as the zwitterionic phase of interest and was further investigated.

Several lots of the form F monohydrate were produced on gram scale, and the form was confirmed by XRPD. However, when the lots were characterized via DSC, they were found to have widely different melting temperatures, ranging from 180 to 187 °C. Such a large shift in the melting point temperature of lots found to be the same phase and of comparable purity was unexpected. Therefore, DSC and TGA ramp rates of 1 and 10 °C/min were used to recharacterize form F (Figure 5). The data showed that the onset temperature of the desolvation and suspect melt endotherms in the DSC curves change significantly as a function of heating ramp rate. This variation indicates that the API is not undergoing a traditional melt (a thermodynamic event) but rather decomposing (a kinetic event). The decomposition was confirmed by TGA and hot stage microscopy.

Although the monohydrated zwitterion form F showed reasonably good physical properties, the zwitterion itself exhibited severe polymorphism and poor water solubility (<4 µg/mL). Thus, a salt screen was conducted in an attempt to identify alternative phases with acceptable physical characteristics suitable for development, a simpler polymorphic profile, and improved solubility.

**Salt Screen.** A salt screen was conducted on **1** ( $pK_a$  2.7 and 8.1) using a variety of counterions including sodium, potassium, and calcium and hydrochloric, phosphoric, sulfuric, acetic, maleic, tartaric, citric, benzoic, malic, malonic, and methanesulfonic acids. Of these salts, the hydrochloric acid, sulfuric acid, and calcium salts appeared to have promising physical properties and were therefore evaluated further.

**HCl Salt.** A polymorph screen was conducted on the hydrochloric acid salt, and two forms were identified (Figures 6 and 7). Form A was found to be a crystalline unsolvated phase whose DSC curve indicated a broad endothermic transition attributed to a melt/decomposition around 188 °C. Water vapor sorption analysis for form A indicated that the material was nonhygroscopic

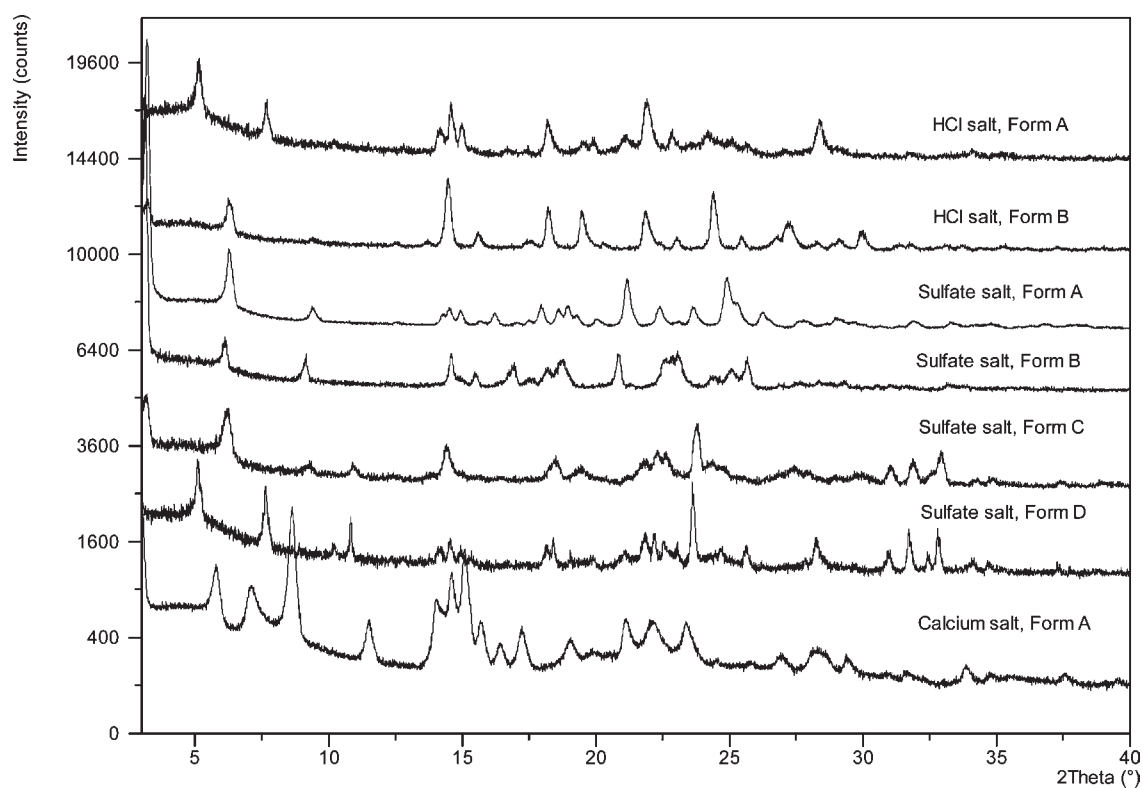


Figure 6. Summary of XRPD patterns for crystalline salts.

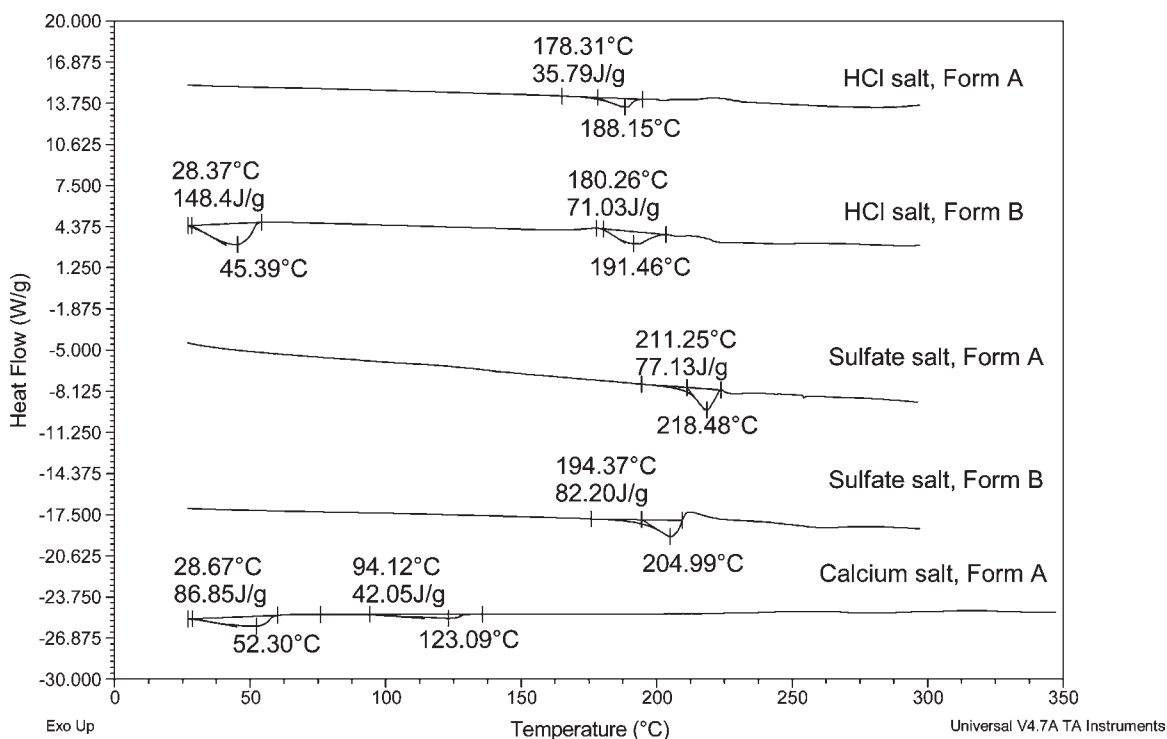


Figure 7. Summary of DSC curves for crystalline salts.

and exhibited a +0.15% weight change as high as at 95% relative humidity. Also, the phase remained unchanged post experiment based on XRPD results. Form B was found to be a crystalline

dihydrate (KF = 6.7 wt %, theoretical 6.8 wt %) whose DSC curve indicated an endothermic transition at 45 °C attributed to desolvation and confirmed by TGA analysis and an endothermic

transition at 191 °C attributed to a melt/decomposition. Water vapor sorption analysis indicated that the form desolvated when dried to 5% relative humidity, but the material fully rehydrates at 15% relative humidity. Above 15% relative humidity, the sample is slightly hygroscopic and exhibited a +0.2% weight change as high as at 95% relative humidity. To understand the desolvation process seen in the vapor sorption curve, form B was heated on a variable temperature X-ray spectrometer. When the material was heated past desolvation temperatures, the sample underwent only very slight changes in the XRPD pattern, attributed to its conversion to an isomorphous dehydrated hydrate. When the material was allowed to cool back to ambient conditions, TGA analysis indicated that it immediately rehydrated to a full dihydrate. This indicated that form B appeared to behave like a channel hydrate, whose water could easily move in and out of the crystal lattice without significantly changing the crystalline structure. Since both forms A and B of the HCl salt appeared to have viable physical properties, the critical water level required for conversion between the two forms was determined in MeOH and found to be around 5% v/v water in a MeOH/water system (the preferred process solvent at the time). This data suggested that the dihydrate was the preferred form since our process conditions were projected to be above the critical water level (4–5% water was used at the start of development with the strong probability of this level being increased).

**Sulfate Salt.** A polymorph screen was conducted on the sulfate salt, and four forms were identified (Figures 6 and 7). Form A was found to be a crystalline unsolvated phase whose DSC curve indicated a broad endothermic transition attributed to melting around 218 °C. Water vapor sorption analysis for form A indicated that the material was slightly hygroscopic and exhibited a +0.3% weight change as high as at 95% relative humidity, and the phase remained unchanged post experiment based on XRPD results. Form B was found to be a crystalline unsolvated phases whose DSC curve indicated a broad endothermic transition attributed to melting around 205 °C. Water vapor sorption analysis was not conducted on this phase, but rather the material was used to perform slurry interconversion investigations. When form B material was slurried in EtOH, MeOH, THF, and water separately at room temperature, it converted to form A, and the data suggested that form A was the room-temperature-stable phase. Form C material was isolated in an attempt to scale form A under process conditions. When form C material was slurried in EtOH and MeOH, it converted to form A, but when it was slurried in MeCN and THF, it converted to a new form (form D).

Because of the increasingly complex nature of the polymorphism of the sulfate salt and the time required to further understand their relationship, the sulfate salt was deprioritized as a form for phase I clinical investigations. However, it was still considered viable for long-term development with the understanding that further work would be required to have the same understanding of the sulfate salt as was known for the zwitterion and HCl salt.

**Calcium Salt.** Only one form of the calcium salt was identified (Figures 6 and 7). It was found to be a crystalline hexahydrate (KF = 10.0 wt %, theoretical 10.1 wt %) whose DSC curve indicated endothermic transitions at 52 and 123 °C, both attributed to desolvation when confirmed by TGA analysis. Approximately 8.5% water was lost in an initial step from 30 to 85 °C, while the remaining 1.5% water was lost in a secondary step from 80 to 160 °C. When the material was partially desolvated by heating to 85 °C, it was found to fully rehydrate

after equilibrating at ambient conditions for 30 min. XRPD analysis of the material post complete desolvation (heated to 160 °C) indicated that the material converted to an amorphous phase. This would suggest that the water in the calcium salt is bound in two different environments (one loosely bound similar to a channel hydrate and one tightly bound) and that the crystalline phase requires the guest water molecules to stabilize the crystal lattice. Water vapor sorption analysis indicated that the material was slightly hygroscopic and exhibited a +1.0% weight change from 45% to 95% relative humidity. When the sample was dried below 45% RH, it was found to lose water (3.25% weight loss at 5% RH), which was resorbed when re-equilibrated to 45% RH. The phase remained unchanged post experiment based on XRPD results.

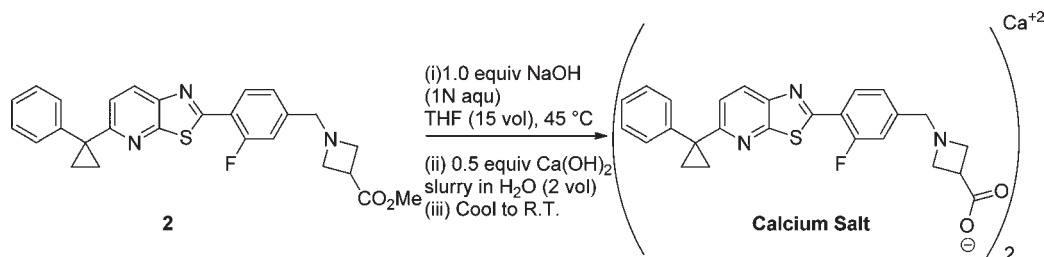
Although the calcium salt was behind in development, it was the only basic salt to have viable physical characteristics. On the basis of the project timeline to support phase I clinical investigations, the calcium salt was too far behind in development to consider but still a potential form to investigate for long-term development.

**Phase Scale-up. Basic Salts.** Basic salts of the zwitterionic **1** were desirable as they could be accessed cleanly and efficiently from the penultimate intermediate 2317157 (**2**) via base-promoted saponification and subsequent crystallization. Although numerous attempts to promote crystallization of a sodium or potassium salt of **1** with suitable properties to advance were met with failure, a promising crystalline calcium salt was identified. The calcium salt of interest could be crystallized starting from a solution of the sodium salt of **1** in 12% v/v water/THF after sodium hydroxide promoted saponification by charging a slurry of 0.5 equiv of Ca(OH)<sub>2</sub> in water (Scheme 1). This procedure to produce the calcium salt of **1** was reproducible on gram scale and allowed for further investigations of the properties of this basic salt.

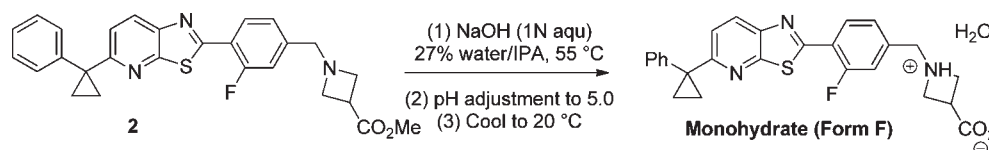
**Neutral Forms.** A process was developed to reliably access the neutral form of interest of the zwitterion, the form F monohydrate, from the penultimate intermediate **2**. Solvents for the saponification were evaluated with aqueous sodium hydroxide for (i) efficiency of the transformation, (ii) crystallinity of the resultant form F hydrate as judged by XRPD, and (iii) tendency to entrap inorganic content during the pH-adjusted reactive crystallization of the hydrate. Although the reaction was complete in less than 1 h in aqueous THF, alcohol solvents such as MeOH or IPA were capable of effecting full conversion of **2** in 4 h or less at 50 °C. Ultimately, development ensued using IPA due to its ICH class 3 status. The water activity of the form F monohydrate was found to be very low with the monohydrate being favored in aqueous alcohol systems containing ≥4% v/v water. However, to facilitate a polish filtration of the intermediate sodium salt of **1**, the amount of water was optimized to 27% v/v. Following filtration, the solution was heated to 55 °C, and the pH was adjusted from 12.9 to 8.0, which was just below the first pK<sub>a</sub>. At this point, the solution was found to hold a 1 wt % seed charge. After establishing a seed bed, the pH of the solution was slowly adjusted to 5.0 with incremental charges of HCl (5 N aqueous), and the mixture was cooled to 20 °C over 6 h. Following this procedure, the form F monohydrate was prepared on kilogram scale in 94% corrected isolated yield (Scheme 2).

**Acidic Salts.** In order to facilitate the scale-up of the acidic salt forms of interest for additional characterization, attempts were made to hydrolyze the methyl ester penultimate intermediate under acidic conditions. Unfortunately, the acid-promoted hydrolysis of **2**

Scheme 1. Gram-Scale Synthesis of the Calcium Salt of 1



Scheme 2. Scale-up of the Monohydrate of 1 (Form F)



Scheme 3. Scale-up of the Synthesis of the Sulfate Salt of 1

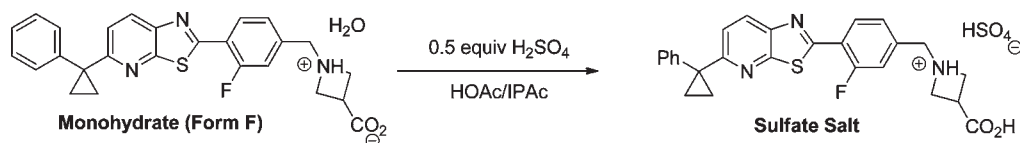


Table 1. Chemical Stability of Phases Stored in Open Vial Conditions at 40 °C/75% RH and 60 °C, 4 Weeks Study Time

	zwitterion		HCl salt		sulfate salt	
	40 °C/ 75% RH	60 °C	40 °C/ 75% RH	60 °C	40 °C/ 75% RH	60 °C
% total impurities	0.28	2.49	1.94	36.53	1.03	1.83

was plagued with incomplete conversion even when excess acid was employed. In an attempt to address this issue, continuous distillation conditions were examined in solvents that form azeotropes with MeOH.<sup>14</sup> Unfortunately, the hydrolysis stalled at  $\leq 95\%$  conversion under the best of these conditions, and under forcing conditions such as elevated temperatures, the growth of additional impurities became a major concern. As such, the acidic final forms of 1 were accessed from the penultimate 2 via a two-step process that involved isolation of zwitterionic 1 after base-promoted hydrolysis of the methyl ester (see above) and then formation of the acidic salt in a separate operation. Although initial lots of the acidic salts were formed via a slurry-to-slurry conversion of zwitterionic 1, HOAc and DMF were later identified as potential solvents with IPAc presenting itself as a suitable antisolvent for isolation of the desired acidic salt forms of interest via crystallization. This process was demonstrated on gram-scale for the synthesis of the sulfate salt of 1 (Scheme 3).

**Chemical Stability.** The zwitterion monohydrate, HCl salt dihydrate, and sulfate salt form A were placed on stability in open-faced vials at 40 °C/75% RH and 60 °C (Table 1). At the 40 °C/75% RH conditions after 4 weeks, all three phases had a

total percent of impurities of less than 2%, with the zwitterion at only 0.28%. However at the 60 °C condition, the HCl salt was found to have up to approximately 36% impurities, while the zwitterion had 2.49% and sulfate salt had 1.83%. Further investigations indicated that the major degradant from the stress investigation was due to acid-catalyzed nucleophilic attack. Because of stability issues, the HCl was deprioritized as a phase of interest, while the calcium salt was further investigated to see if a basic salt could avoid this degradation process. Although the sulfate salt showed stability similar to that of the zwitterion, it still required work to map the relationship of the various phases, and therefore focus was placed on the zwitterion and the calcium salt.

A portion of the good manufacturing procedures (GMP) batch of the monohydrate of the zwitterion and a development batch of the hexahydrate calcium salt were placed on stability to monitor the growth of the major degradant. The data are summarized in Table 2 and indicate that, at all three conditions tested, the zwitterion showed an increase in the acid-catalyzed substitution degradant after 2 months, while the calcium salt showed no change in the level at 40 °C/75% RH condition. On the basis of these results, the storage conditions for the zwitterion monohydrate bulk drug substance were revised from room temperature to 2–8 °C. Also, the calcium salt was shown to not suffer from the acid-catalyzed nucleophilic attack stability issue and thus was considered a phase worth further pursuing for long-term development.

**Form Selection.** In order to determine which phase should be recommended for phase I clinical testing and/or long-term development, the following quality attributes were compared: hygroscopicity, crystallinity, API stability, API scale-up, drug product (tablet) manufacturability, solubility and PK exposure

(Table 3). All phases were found to be crystalline and slightly hygroscopic. With respect to stability, the zwitterion and HCl and sulfate salts suffered from acid-catalyzed substitution, and storage conditions were set to under refrigeration, while the calcium salt appeared to not suffer from this stability issue. Manufacture of the zwitterion and HCl and calcium salts was scalable, while the sulfate salt required further work to understand the thermodynamic relationship between the various polymorphs to ensure control of the correct phase during scale-up. It appeared feasible to use either wet granulation or a dry process for the zwitterion and HCl and calcium salts for tablet manufacture because these phases are hydrated phases that upon dehydration have been shown to rehydrate under ambient conditions. Further work was needed to screen the sulfate salt for hydrated phases we may not have yet identified, which might create problems when performing a wet granulation process on an unsolvated phase. The zwitterion and all salts were found to have poor water solubility ( $<4 \mu\text{g}/\text{mL}$ ), and while PK data for the sulfate and calcium salt were not collected at the time, a suspension of the HCl salt was found to have an area under the concentration–time curve from time zero to infinity ( $\text{AUC}_{0-\infty}$ ) 38% higher than that of a suspension of the zwitterion and 10% higher than that of a solution of the zwitterion in rat at 1 mg/kg.

In summary, due to the superior properties of the monohydrate (form F) of the zwitterion relative to the HCl, sulfate, and calcium salts, it was recommended for phase I clinical investigations. However, since this phase needed to be stored under refrigeration conditions to inhibit degradation in the solid

state, the Ca salt is still under consideration for long-term development.

## CONCLUSIONS

A polymorph and salt screen was conducted on **1**. Several phases were identified including a monohydrate of the zwitterion, a dihydrate of the HCl salt, unsolvated sulfate salt, and a hexahydrate of the calcium salt. Although several of these phases appeared to be viable for development, ultimately the hydrated form of the zwitterion was recommended for phase I clinical investigations because it was a crystalline, slightly hygroscopic phase that was scalable and preliminary investigations indicated it was amenable to tablet manufacturing. However, because the monohydrate of the zwitterion showed a propensity to undergo low level degradation at ambient conditions, the calcium salt was selected as a backup and a potential replacement candidate for long-term development.

## EXPERIMENTAL SECTION

All water used was distilled twice and deionized.

X-ray powder diffraction (XRPD) patterns were collected using a Phillips X-ray automated powder diffractometer (X'Pert). Diffraction patterns were collected at room temperature between  $3^\circ$  and  $40^\circ 2\theta$  with a step size of  $0.008^\circ$  and a counting time of 15.24 s. Instrument voltage was 45 kV, and the current was 40 mA. Data analysis was performed utilizing X'Pert Data Viewer 1.2, PANalytical. Variable temperature XRPD patterns were collected with a heating stage chamber accessory using the instrumental parameters described above. Sample was held at each temperature for approximately 5 min.

Differential scanning calorimetry traces were produced by loading powder samples (1–5 mg) into open aluminum DSC pans and characterized on either a TA Instruments Q 100 or Q 1000. Data analysis was performed utilizing Universal Analysis 2000, TA Instruments. A heating rate of 1 or  $10^\circ\text{C}/\text{min}$  was used over a variety of temperature ranges.

Thermogravimetric analysis was performed on samples using a TA Instruments Q 500. A heating rate of 1 or  $10^\circ\text{C}/\text{min}$  was used over a variety of temperature ranges. Data analysis was performed utilizing Universal Analysis 2000, TA Instruments.

**Table 2. Chemical Stability Monitoring Acid-Catalyzed Substitution Impurity in the Zwitterion and Calcium Salt**

time point	stress condition	% impurity of major degradant in zwitterion	% impurity of major degradant in calcium salt
0	NA	0.01	0.11
2 months	25 °C/60% RH	0.06	NA <sup>a</sup>
	30 °C/65% RH	0.09	NA <sup>a</sup>
	40 °C/75% RH	0.20	0.11

<sup>a</sup> Not available.

**Table 3. Comparison of Phases of Interest**

	zwitterion form F, monohydrate	HCl salt form B, dihydrate	sulfate salt form A, unsolvated	calcium salt form A, hexahydrate
hygroscopicity	slightly hygroscopic	slightly hygroscopic	slightly hygroscopic	slightly hygroscopic
crystallinity	crystalline	crystalline	crystalline	crystalline
API stability	degradation via acid-catalyzed substitution, storage conditions under refrigeration	degradation via acid-catalyzed substitution, less stable than other phases of interest	degradation via acid-catalyzed substitution, storage conditions under refrigeration	good stability, no degradation via acid-catalyzed substitution
API manufacture	scalable	scalable	more work required to understand various phases	scalable
tablet manufacture	feasible to use wet granulation or dry process	feasible to use wet granulation or dry process	more work required to understand formulation challenges	feasible to use wet granulation or dry process
solubility	$<4 \mu\text{g}/\text{mL}$	$<4 \mu\text{g}/\text{mL}$	$<4 \mu\text{g}/\text{mL}$	$<4 \mu\text{g}/\text{mL}$
PK data	PK/BA profile in rat (1 mg/kg dose), HCl suspension was 38% higher than zwitterion suspension and 10% higher than zwitterion solution.		NA <sup>a</sup>	NA <sup>a</sup>

<sup>a</sup> Not available.

Dynamic vapor sorption data were collected at 25 °C using a VTI SGA 100 symmetrical vapor sorption analyzer. Relative humidity was varied in increments of 5%, starting at 5% relative humidity, increasing to 95% relative humidity, and then undergoing a drying cycle back to 5% relative humidity. Equilibrium criteria were set at 0.01% weight change in 1 min with a maximum equilibrium time of 180 min. Approximately 1–5 mg of sample was used.

Karl Fischer titrations were performed using a Mettler Toledo C20 Coulometric KF titrator filled with Aquastar CombiCoulomat Methanol Solution. Approximately 20–30 mg of sample was used for analysis.

HPLC for solubility measurements was run using an Agilent Series 1100 having a Phenomenex Luna C18 column (30 × 4.60 mm, 3 μm). Analyses were run with a gradient method using 98% water 2% acetonitrile (mobile phase A) and 98% acetonitrile 2% water (mobile phase B) with a gradient going from 10% to 95% B at a flow rate of 1 mL/min and a total run time of 5 min. UV detection was run at a wavelength of 254 nm.

HPLC for stability samples was run using an Agilent Series 1100 having a Bonus RP column (3 mm × 150 mm, 3.5 μm). Analyses were run with a gradient method using 90% water 10% methanol with 0.05% trifluoroacetic acid (mobile phase A) and 40% acetonitrile 60% methanol with 0.05% trifluoroacetic acid (mobile phase B) with a gradient going from 10% to 85% B at a flow rate of 0.6 mL/min and a total run time of 57 min. UV detection was run at a wavelength of 324 nm.

**Polymorph and Salt Screening.** Recrystallization experiments included evaporation, slurries, antisolvent addition, and heating experiments. Evaporation experiments were conducted by dissolving approximately 5–10 mg of the API in a given solvent, filtering the solution with a 0.45 μm PTFE filter into a vial, then either leaving the vial uncovered or covering the vial with pin-holed Parafilm to dry. Slurry experiments were performed by saturating a giving solvent with API, such that excess solid was in constant contact with solution. The sample was then agitated on a slurry wheel at room temperature for approximately 1 week. Antisolvent addition experiments were performed by dissolving a portion of the API in 1 mL of solvent followed by addition of 25 mL of antisolvent and then cooling the solution in a refrigerator. Solids from slurry and antisolvent addition experiments were isolated via suction filtration and allowed to air-dry.

**Solubility Measurements.** Solubility measurements ( $n = 1$ ) were conducted by saturating a given solvent system with API at a given temperature, and agitating the mixture for 24 h. The suspension was then filtered using a PTFE (0.45 μm) filter. The resulting solid phase was examined via XRPD, while the resulting solution was analyzed for drug concentration via HPLC. For each experiment, no phase change or salt disproportionation was observed.

## ■ ASSOCIATED CONTENT

Supporting Information. Further experimental data. This material is available free of charge via the Internet at <http://pubs.acs.org>.

## ■ AUTHOR INFORMATION

### Corresponding Author

\*Ph: 805-313-5502. Fax: 805-498-8674. E-mail: [hmorriso@amgen.com](mailto:hmorriso@amgen.com).

## ■ ACKNOWLEDGMENT

The authors thank Matthew Noestheden and Darren Reid for the supporting forced degradation data and Yang Xu for the supporting PK data for these investigations.

## ■ NOTATION

MeOH = methanol; EtOH = ethanol; THF = tetrahydrofuran; MeCN = acetonitrile; IPA = isopropanol; HOAc = acetic acid; DMF = dimethylformamide; IPAc = isopropyl acetate

## ■ REFERENCES

- (1) Cee, V. J.; Frohn, M.; Lanman, B. A.; Golden, J.; Muller, K.; Neira, S.; Pickrell, A.; Arnett, H.; Buys, J.; Gore, A.; Fiorino, M.; Horner, M.; Itano, A.; Lee, M. R.; McElvain, M.; Middleton, S.; Schrag, M.; Rivenzon-Segal, D.; Vargas, H. M.; Xu, H.; Xu, Y.; Zhang, X.; Siu, J.; Wong, M.; Burlin, R. W. *ACS Med. Chem. Lett.* **2011**, *2* (2), 107–112.
- (2) Rosen, H.; Gonzalez-Cabrera, P. J.; Sanna, M. G.; Brown, S. *Annu. Rev. Biochem.* **2009**, *78*, 743–768.
- (3) Takabe, K.; Paugh, S. W.; Milstien, S.; Spiegel, S. *Pharmacol. Rev.* **2008**, *60*, 181–195.
- (4) Salvadori, M.; Budde, K.; Charpentier, B.; Klempnauer, J.; Nashan, B.; Pallardo, L. M.; Eris, J.; Schena, F. P.; Eisenberger, U.; Rostaing, L.; Hmissi, A.; Aradhye, S. *Am. J. Transplant.* **2006**, *6*, 2912–2921.
- (5) Kappos, L.; Radue, E. W.; O'Connor, P.; Polman, C.; Hohlfeld, R.; Calabresi, P.; Selmaj, K.; Agoropoulou, C.; Leyk, M.; Zhang-Auberson, L.; Burtin, P. *New Engl. J. Med.* **2010**, *362*, 387–401.
- (6) Cohen, J. A.; Barkhof, F.; Comi, G.; Hartung, H. P.; Khatri, B. O.; Montalban, X.; Pelletier, J.; Capra, R.; Gallo, P.; Izquierdo, G.; Tiel-Wilek, K.; de Vera, A.; Jin, J.; Stites, T.; Wu, S.; Aradhye, S.; Kappos, L. *New Engl. J. Med.* **2010**, *362*, 402–415.
- (7) Gould, P. L. *Int. J. Pharm.* **1986**, *33*, 201–217.
- (8) Bastin, R. J.; Bowker, M. J.; Slater, B. J. *Org. Process. Res. Dev.* **2000**, *4*, 427–435.
- (9) Stahl, P. H.; Wermuth, C. G. *Handbook of Pharmaceutical Salts: Properties, Selection and Use*; Helvetica Chimica Acta: Zurich, 2002.
- (10) Gross, T. D.; Schaab, K.; Ouellette, M.; Zook, S.; Reddy, J. P.; Shurtleff, A.; Sacca, A. I.; Aebic-Kolbah, T.; Bozigian, H. *Org. Process Res. Dev.* **2007**, *11*, 365–377.
- (11) Maurin, M. B.; Rowe, S. M.; Koval, C. A.; Hussain, M. A. *J. Pharm. Sci.* **1994**, *83* (10), 1418–1420.
- (12) Kumar, L.; Amin, A.; Bansal, A. K. *Pharm. Technol.* **2008**, *3* (32), 128–146.
- (13) Morrison, H.; Jona, J.; Walker, S. D.; Woo, J. C. S.; Li, L.; Fang, J. *Org. Process Res. Dev.* **2011**, *15* (1), 104–111.
- (14) Methanol is the biproduct of hydrolysis of 2317157 with acid; therefore, acetonitrile, tetrahydrofuran, toluene, and isopropyl acetate were screened as solvents for the hydrolysis under these conditions.